

## Original Article

**Cite this article:** Zhou Z, Ding W, Zhang R, Xue M, Jiao B, Wu C, Chen Y, Qiu L, Du X, and Liu T (2022) Structural styles and tectonic evolution of Mesozoic–Cenozoic faults in the Eastern Depression of Bayanhaote Basin, China: implications for petroleum traps. *Geological Magazine* **159**: 689–706. <https://doi.org/10.1017/S0016756821001242>

Received: 28 April 2021

Revised: 5 November 2021

Accepted: 5 November 2021

First published online: 20 January 2022

### Keywords:

fault activity; structural style; tectonic evolution; petroleum trap; Bayanhaote Basin

### Author for correspondence:



Wenlong Ding,

Email: [Dingwenlong2006@126.com](mailto:Dingwenlong2006@126.com);

Ruifeng Zhang,

Email: [ktb\\_zrf@petrochina.com.cn](mailto:ktb_zrf@petrochina.com.cn)

# Structural styles and tectonic evolution of Mesozoic–Cenozoic faults in the Eastern Depression of Bayanhaote Basin, China: implications for petroleum traps

Zhicheng Zhou<sup>1,2,3</sup> , Wenlong Ding<sup>1,2,3</sup>, Ruifeng Zhang<sup>4</sup>, Mingwang Xue<sup>5</sup>, Baocheng Jiao<sup>1,2,3</sup>, Chenlin Wu<sup>6</sup>, Yuting Chen<sup>7</sup>, Liang Qiu<sup>8</sup> , Xiaoyu Du<sup>1,2,3</sup> and Tianshun Liu<sup>1,2,3</sup>

<sup>1</sup>School of Energy Resources, China University of Geosciences, Beijing 100083, China; <sup>2</sup>Beijing Key Laboratory of Unconventional Natural Gas Geology Evaluation and Development, China University of Geosciences, Beijing 100083, China; <sup>3</sup>Key Laboratory of Strategy Evaluation for Shale Gas, Ministry of Natural Resources of the People's Republic of China, China University of Geosciences, Beijing 100083, China; <sup>4</sup>PetroChina Huabei Oilfield Company, Renqiu 062550, China; <sup>5</sup>Tianjin Branch of China National Offshore Oil Company Ltd, Tianjin 300452, China; <sup>6</sup>Bayan Exploration and Development Branch, PetroChina Huabei Oilfield Company, Bayannur 015300, China; <sup>7</sup>Research Institute of Exploration and Development, PetroChina Huabei Oilfield, Renqiu 062550, China and <sup>8</sup>School of Earth Sciences and Resources, China University of Geosciences, Beijing 100083, China

## Abstract

The Eastern Depression in the Bayanhaote Basin in western Inner Mongolia has experienced multi-stage Meso-Cenozoic tectonic events and possesses considerable exploration potential. However, structural deformation patterns, sequences and the genesis of oil-bearing structures in the basin are still poorly understood. In this study, based on high-quality 2D seismic data and drilling and well-logging data, we elucidate the activities and structural styles of faults, the tectonic evolution and the distribution characteristics of styles, as well as assessing potential petroleum traps in the Eastern Depression. Five types of faults that were active at different stages of the Meso-Cenozoic faults have been recognized: long-lived normal faults active since the late Middle Jurassic; reverse faults and strike-slip faults active in the late Late Jurassic; normal faults active in the Early Cretaceous; normal faults active in the Oligocene; and negative inverted faults active in the Early Cretaceous and Oligocene. These faults constituted 12 geometric styles in NE-trending belts at various stratigraphic levels, and were formed by compression, strike-slip, extension and inversion. The temporal development of structural styles promoted the formation and reconstruction and finalization of structural traps, while regional unconformities and open reverse and strike-slip faults provided migration pathways for petroleum to fill the traps. In general, potential traps that formed by compressional movement and strike-slip movement in the late Late Jurassic are primarily faulted anticlines. Those traps developed in Carboniferous rocks and are located in the southwestern region of the Eastern Depression, being controlled by NNE-NE-striking reverse and transpressive faults.

## 1. Introduction

Structural style refers to the specific combination of structures that have a close connection with each other in terms of profile shapes, plane layouts, arrangements and response mechanisms. Such structures have similar structural characteristics and deformational mechanisms (Yang, 2006; Missenard *et al.* 2007; Tripodi *et al.* 2013; Saqab & Bourget, 2015). The increasing relevance of structural-style-controlled petroleum traps to exploration in deeper basins has increased interest in deciphering how the structural style influences the basin formation and filling process (Harding & Lowell, 1979; Allen *et al.* 1997; Polonia & Camerlenghi, 2002; Sepehr & Cosgrove, 2004; Hickman *et al.* 2009). The structural style and generation reveal the deformation sequence accompanying transitions between tectonic regimes, which produces petroleum traps and causes the migration of petroleum into structural traps within sedimentary basins (Nieuwland *et al.* 2001; Sherkatia & Letouzey, 2004; Zhou *et al.* 2021). In several basins in China, both the pattern of subsidence with burial sedimentation and subsequent deformation were dominantly influenced by regional tectonics or the basement structural style (Yao *et al.* 2004; Zhang *et al.* 2014; Cheng *et al.* 2016; Fan *et al.* 2020; Xu & Gao, 2020). Therefore, a comprehensive analysis of structural style and sequence is necessary to understand the tectonic pattern and inversion of these basins, which in turn provide a geological basis for petroleum exploration.

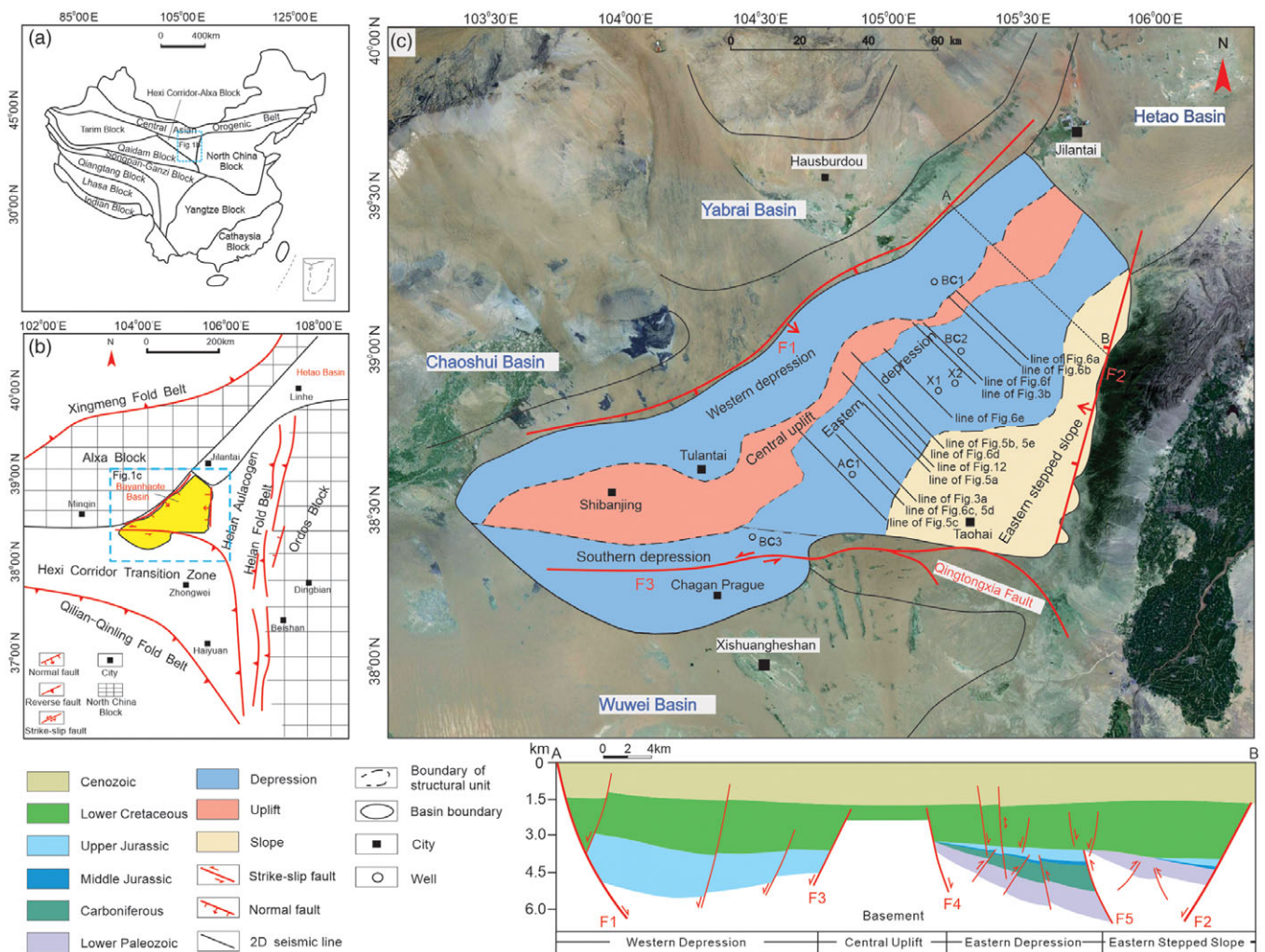


**Fig. 1.** (Cenozoic) (a) Geotectonic zoning of China and location of the Bayanhaote Basin. (b) Sketch map of the Bayanhaote Basin and adjacent tectonic zones. (c) Map of the structural units of the Bayanhaote Basin superimposed on a remote-sensing image of the region (modified from Song *et al.* 1999). Also shown are the location of the study area (Eastern Depression), boundary faults (F1 – Bayanwula Mountain Fault; F2 – Helan Fault; F3 – Chahan Fault) and the seismic profiles used in this study. The geological profile along line AB across the northwestern Bayanhaote Basin shows the present structural and stratigraphic architecture of the Western Depression, Eastern Depression and the Eastern Stepped Slope.

The Bayanhaote Basin, in the western portion of Inner Mongolia, China, is located in the eastern Alxa Block, adjacent to the Helan Fold Belt to the east and the Hexi Corridor Transition Zone to the south (Xiong *et al.* 2001; Fig. 1). Occupying an area of 18 000 km<sup>2</sup>, the Bayanhaote Basin has accumulated thick sequences of Early Palaeozoic marine sediments, Late Palaeozoic interactive marine–continental sediments and Meso-Cenozoic continental sediments and is an area that has extremely high hydrocarbon potential. The Bayanhaote Basin is a complex superimposed basin; the Southern Depression was a foreland basin derived from the Early Palaeozoic bell-mouth bay, the Eastern Depression was a rift basin derived from the Early Palaeozoic aulacogen and the Western Depression was a strike-slip pull-apart basin. The whole basin subsided and was overlain by Cretaceous sediments forming a unified basin by the end of the Early Cretaceous (Tang *et al.* 1990; Liu, 1997a; Xiong *et al.* 2001). This tectonic configuration resulted in a complex structural pattern consisting of alternately distributed uplifts and depressions within the Bayanhaote Basin. These uplifts and depressions are characterized by both extensional and compressional deformation, as well as strike-slip deformation and tectonic

inversion (Tang *et al.* 1990; Liu, 1997a; Song *et al.* 1999; Xiong *et al.* 2001; Xue *et al.* 2020).

Owing to insufficient geological data, the tectonic framework, genesis and evolution of the Bayanhaote Basin are subjects of debate. For instance, some scholars propose that the Bayanhaote Basin formed due to Mesozoic–Cenozoic faulting subsidence and that it is developed above different crystalline basements. They argue that the basin and its surrounding areas have experienced five tectonic episodes from the Early Proterozoic to the Cenozoic, namely, the formation of the Early–Middle Proterozoic ‘Qin-Qi-He’ triangulated rift, the Late Proterozoic–Ordovician aulacogen, the Silurian–Devonian foreland basin, the Carboniferous–Permian composite basin and the Meso-Cenozoic faulting-subsidence basin (Tang *et al.* 1990; Song *et al.* 1999; Xiong *et al.* 2001). However, Tang *et al.* (1990) interpreted the structures in the Bayanhaote Basin as being mainly normal faults with a few reverse faults and folds, while Liu (1994) and Liu & Liu (2002) claimed that the structures in the basin were represented by both extensional and compressional structures, including shovel-type normal faults, horst–graben blocks and traction folds in the Western Depression, and imbricate thrust

faults and back-thrust faults in the Southern and Eastern Depressions, and Song *et al.* (1999) proposed that some flower structures were controlled by the Chahan sinistral strike-slip fault in the Southern Depression. Still other scholars have suggested that the Bayanhaote Basin was a Mesozoic–Cenozoic strike-slip pull-apart basin and was controlled by a sinistral strike-slip movement of the western Bayanwula Mountain Fault during the late Middle Jurassic – early Early Cretaceous and a dextral strike-slip movement of the fault during the Cenozoic, with weak inversion of early thrust faults during the Late Jurassic (Xue *et al.* 2020). The core of the debate is how the types of structural styles and their temporal development within the basin influenced the formation and subsequent deformation of the basin. In addition to clarifying this aspect, a comprehensive analysis of structural styles will help elucidate the temporal and spatial relationship of potential structural traps, thereby accelerating oil exploration.

The Eastern Depression has the greatest oil-bearing potential in the Bayanhaote Basin, as it contains widely distributed Carboniferous source rocks. With increasing oil and gas exploration in this area, it is important to improve the characterization of the structural and stratigraphic architecture of the depression and their local effects on hydrocarbon trapping. However, owing to the limited availability of early seismic and drilling data, only a few detailed analyses of the structural styles of faults and the distribution of petroleum traps have been carried out in the Eastern Depression. Furthermore, a poor identification of geometric and kinematic styles has led to a poor understanding of the formation of trap structures and petroleum migration. In this work, based on a new comprehensive understanding of drilling and logging data and a number of high-quality 2D seismic profiles, we analyse the activities and structural styles of Meso-Cenozoic faults, focusing on the tectonic evolution and distribution characteristics of the styles in this region, so as to elucidate the control exerted by the structures formed by different mechanisms on trap formation and petroleum accumulation and to describe the locations of potential petroleum traps.

## 2. Geological setting

The Bayanhaote Basin is located at the junction of the Alxa Block, the Helan Fold Belt and the Hexi Corridor Transition Zone (Fig. 1b; Xiong *et al.* 2001). The basin is roughly triangular in form, being narrower in the north and wider in the south, with an area of  $1.8 \times 10^4 \text{ km}^2$  (Tang *et al.* 1990; Liu, 1994; Liu & Liu, 2002). The Alxa Block in the northwestern part of the basin is an Archaeozoic micro-block surrounded by orogenic belts and fault zones, and was separated from the Ordos Block in the east during the Meso-Neoproterozoic. The Palaeozoic, Jurassic–Cretaceous and Cenozoic strata are well developed in the Alxa Block (Song *et al.* 1999; Xiong *et al.* 2001). The Helan Fold Belt is a NNE–SSW-striking tectonic belt located in the eastern part of the basin; it is sandwiched between the Alxa Block and the Ordos Block. It consists of multi-stage deformed Precambrian basement rocks overlain by Cambrian–Jurassic covers. Carboniferous–Permian marine carbonate and clastic deposits outcrop in the central and northern parts of the Helan Mountains (Liu, 1998; Liu *et al.* 2010). The Hexi Corridor Transition Zone in the southern part of the basin refers to the transitional zone between the North Qilian Orogenic Belt and the Alxa Block (Tang *et al.* 1990). In response to the collision of the North China Block and the Central Qilian Block and the ensuing orogeny during the Silurian–Devonian, Silurian flysch deposits and

Devonian molasse deposits are widely developed in the North Qilian – Hexi Corridor areas (Zhao *et al.* 2016).

The basement of the basin can be divided into three major segments (Tang *et al.* 1990; Liu, 1994; Liu & Liu, 2002; Gao & Wang, 2011). The northern segment, which is bounded by the Zhuoertao–Qingshan fault at the eastern margin of the Middle Uplift, is composed of crystalline metamorphic rocks of the Alxa Group. The southern segment, which is bounded by the Chahan Fault (F3) to the north, is made up of epimetamorphic rocks of the Hexi Corridor Transition Zone. The eastern segment comprises non-metamorphic sedimentary rocks of the Helan Fold Belt. The basin is controlled by three boundary faults, namely, the Bayanwula Mountain Fault (F1), the Helan Fault (F2) and the Chahan Fault (F3). The Bayanwula Mountain Fault (F1) is a SE-dipping, NE–SW-trending normal fault in the northwest. The Helan Fault (F2) is a NW-dipping, N–S-trending normal fault in the east, and the Chahan Fault (F3) is an E–W-trending sinistral strike-slip fault in the south (Fig. 1c).

The Bayanhaote Basin is a superimposed basin that has undergone multiple stages of evolution, including the Meso-Neoproterozoic Qin–Qi–He triangulated rift, the Cambrian–Ordovician aulacogen basin, the Silurian–Devonian foreland basin, the Carboniferous–Permian composite basin, the Mesozoic faulting-subsidence basin and the Cenozoic down-warping basin (Tang *et al.* 1990; Liu & Liu, 1997; Song *et al.* 1999; Xiong *et al.* 2001). The multi-stage tectonic movements occurring during the Late Sinian, Late Cambrian, Late Ordovician, Triassic, Late Jurassic, Late Cretaceous and Neogene modified the basin considerably. According to the deformation framework and stratal distribution pattern, the basin can be divided into five first-order structural units: the Western Depression, the Middle Uplift, the Southern Depression, the Eastern Depression and the Eastern Stepped Slope (Liu, 1994; Fig. 1c). The study area is located in the Eastern Depression at the centre of the basin. It is c. 160 km long and 40–100 km wide and occupies an area of  $>6000 \text{ km}^2$ ; it comprises the main sedimentary depression and oil- and gas-bearing area.

Drilling wells in the basin and outcrops around the basin reveal that the sedimentary rocks of the basin consist of Cambrian strata, Lower and Middle Ordovician strata, the Lower Carboniferous Chouniugou Formation, Upper Carboniferous Jingyuan and Yanghugou formations, Middle Jurassic Zhiluo Formation, Upper Jurassic Fenfanghe Formation, Lower Cretaceous Bayanhaote Group and Palaeogene and Quaternary strata, from bottom to top (Fig. 2). The Cambrian strata are  $>1500 \text{ m}$  thick and consist of carbonate rocks that are mainly exposed in the eastern region of the basin and in the Helan Mountains. The Ordovician strata are  $>1100 \text{ m}$  thick and consist of lower limestone interbedded with mudstone and upper conglomerate interbedded with quartz sandstone; they are observed in wells X1, BC2 and BC3. The Carboniferous strata are  $>1100 \text{ m}$  thick and are mainly composed of mudstone and siltstone mixed with thin coal seams and bioclastic limestone; these strata develop good source rocks and reservoirs. The Mesozoic rocks include Jurassic mudstone, sandstone, and interbedded sandy conglomerate and Cretaceous mudstone, sandy mudstone and arkose. The Middle Jurassic Zhiluo Formation is c. 100 m thick; it is only seen in well BC2 and mainly occurs in the Eastern Depression and in the eastern part of the basin. The Upper Jurassic Fenfanghe Formation is  $>280 \text{ m}$  thick and varies greatly in thickness horizontally. The Cretaceous Bayanhaote Group is  $>1850 \text{ m}$  thick; this group fills in the entire Bayanhaote Basin. The thickness of the Palaeogene strata is c. 500 m, and they consist of interbedded sandstone and conglomerate and dolomitic mudstone. The Quaternary



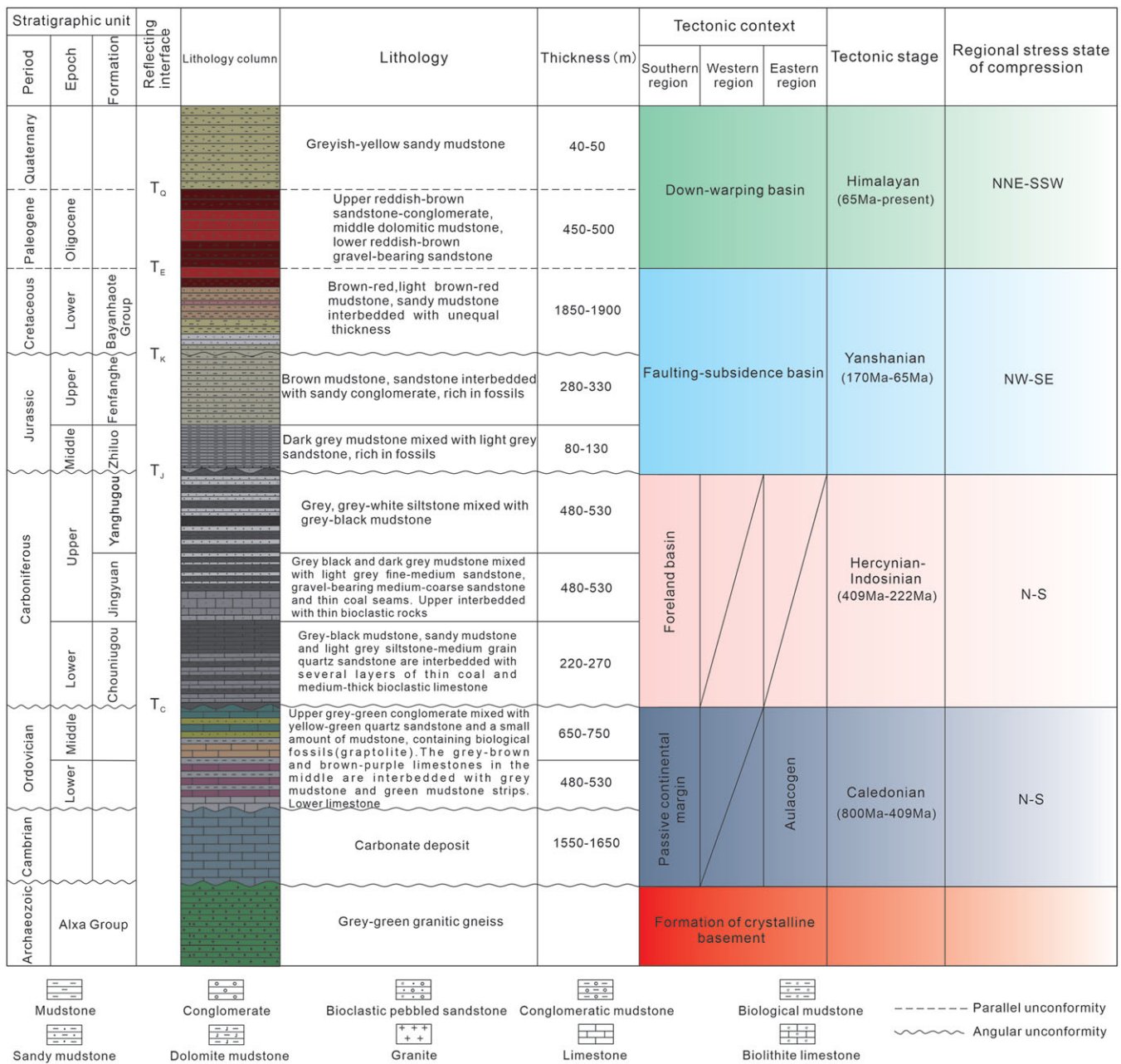


Fig. 2. (Colour online) Comprehensive stratigraphic column of the Eastern Depression, Bayanhaote Basin, showing the lithology, unconformities, tectonic context and stages, and stress state (cited from Tang *et al.* 1990; Yang & Dong, 2018; Ma & He, 2019) of the basin at different tectonic stages.

strata are thin and are composed of sandy mudstone and clay rocks. Four unconformities can be clearly identified from the seismic profiles in the study area, including two angular unconformities, one each between the Upper Carboniferous and Middle Jurassic and between the Upper Jurassic and Lower Cretaceous, and two parallel unconformities, one each between the Lower Cretaceous and Palaeogene and between the Palaeogene and Quaternary.

Hydrocarbon exploration has been underway in the Bayanhaote Basin since the 1950s. The main exploration intervals have changed from the Jurassic strata in the early decades to the Carboniferous strata at present. The latter are composed of a series of marine carbonate rocks and marine-continental interlayered coal-bearing clastic rocks. Six wells, BC1, BC2, BC3, AC1, X1

and X2, have been drilled in the basin, with no commercial oil or gas discoveries in the Carboniferous strata, although hydrocarbon shows with different degrees have been found in wells BC2, BC3 and X1 (Gao & Wang, 2011). Numerous large-scale gas fields have been found in the Carboniferous-Permian strata in the adjacent Ordos Basin (Zhou *et al.* 2014). Moreover, a significant hydrocarbon discovery has recently been made in the Carboniferous-Permian strata in the Yin'E Basin to the north of the Bayanhaote Basin (Lu *et al.* 2011). Although there has not been an industrial breakthrough, the Carboniferous strata have been proved to have source rocks and reservoir conditions that are relatively favourable for hydrocarbon generation; these strata possess great potential for further hydrocarbon exploration in the Eastern Depression of the Bayanhaote Basin

(Wei & Tan, 2009; Gao & Wang, 2011; Wang & Huang, 2014; Li *et al.* 2017; Sheng, 2019). Recent studies have proved that dark mudstones, limestones and coal are the main source rocks that have developed in the Eastern Depression with good oil generation indicators. The total organic carbon (TOC) content of the dark mudstone is 0.14–22.64 %, and the vitrinite reflectance ( $R_o$ ) exceeds 1 % (Wei & Tan, 2009; Li *et al.* 2017). The reservoir lithology mainly consists of interbedded sandstone, grey-black mudstone and grey-shale siltstones, with the average porosity being 5.77 % and the average permeability being  $0.75\text{--}2.2 \times 10^{-3} \mu\text{m}^2$  (Wang & Huang, 2014; Sheng, 2019).

### 3. Materials and methods

In this study, 2D seismic reflection data with a length of >1000 km, mainly obtained from the southwestern part of the Bayanhaote Depression, were used. Drilling data and logging data from four wells were used to calibrate the seismic interpretation. Both datasets were provided by the PetroChina Huabei Oilfield Company. The seismic synthetic records from the four wells were used to guide interpretation of faults and folds and to define a number of stratigraphic units. These seismic data provided information about the characteristics and structural styles of the Mesozoic–Cenozoic faults in the internal depressions.

Previous structural styles from different periods in this work were defined according to the active periods and formation periods of the faults that gave rise to them. The active periods of normal faults were defined mainly according to the syn-sedimentary faults and the upper and lower limits of faults that cut strata, while the formation periods of reverse faults were determined by combining the cross-cutting relationship of faults and strata and unconformities that represented regional compression events. The analysis of inverted faults was mainly based on the upper and lower limits of fault displacements. A regional geological section was generated across the northwestern Bayanhaote Basin by linking a local seismic profile across the Western Depression from Liu (1994) and another seismic profile across the northern Eastern Depression. A step-by-step tectonic restoration was conducted to help better understand the Mesozoic–Cenozoic tectonic evolution of the Eastern Depression and its adjacent tectonic units. Finally, the petroleum generation–migration characteristics and the structural traps formed by different structural styles were analysed, and the locations of potential petroleum traps in the Carboniferous rocks were predicted.

### 4. Active periods and structural styles of Mesozoic–Cenozoic faults

Seismic and drilling data indicated that the Triassic strata were generally absent throughout the Bayanhaote Basin and that the Carboniferous–Permian strata were strongly denuded. The residual Carboniferous strata were only distributed in the Eastern Depression and in the northern portion of the Southern Depression. Moreover the Carboniferous strata were unconformably overlain by the Middle–Upper Jurassic strata, indicating the effects of the Permian–Triassic Indosinian orogenic event. During this period, the northern and southern margins of the basin were compressed by the Xingmeng Fold Belt and the Qilian Fold Belt, respectively; strong uplifting, denudation and folding–thrusting occurred during the period (Tang *et al.* 1990; Liu, 1994; Song *et al.* 1999; Gao & Wang, 2011). Thus, the Carboniferous strata may have been strongly folded by

near-E–W–striking thrusting in the northern and southern regions of the basin during the Permian–Triassic Period. However, no seismic evidence of such faults could be found on the NE-trending seismic profiles used in this study. Therefore, we have only discussed the Mesozoic–Cenozoic faults that significantly influenced the formation of traps and hydrocarbon accumulation.

#### 4.1. Active periods of the Mesozoic–Cenozoic faults

Detailed 2D seismic profile interpretations (Fig. 3) indicate that high-dip-angle normal faults, reverse faults, strike-slip faults and inverted faults were developed in the Eastern Depression. These faults strike NNE in the north, and strike NE in the southward direction. The faults in the Eastern Depression can be subdivided into large-scale level 2 faults that control the boundary of the depression; medium-scale level 3 faults; and small-scale level 4 faults. These faults are characterized by various scales and multi-phase activities and constitute different structural styles according to their geometric and kinematic characteristics (Fig. 4).

##### 4.1.1. Long-lived normal faulting since the late Middle Jurassic

Two long-lived normal faults can be identified in the selected profiles (see F3 and F4 in Fig. 1 and F4 in Fig. 3b). These two normal faults dip to the NW and SE, respectively, forming a horst. They are the western and eastern boundaries of the Central Uplift and delineate a wide segment of the Central Uplift in the northwestern part of the Eastern Depression (Fig. 1). The faults cut the Lower Palaeozoic, Carboniferous, Middle–Upper Jurassic, Lower Cretaceous and Palaeogene strata; the Carboniferous–Jurassic strata in the Eastern Depression horizontally terminate at the hanging wall of the SE-dipping normal fault, that is, the Carboniferous–Jurassic strata are absent in the ascending plate of the faults and are directly structurally overlain by a thin layer of Cretaceous strata. Meanwhile, the Lower Cretaceous strata on the hanging walls of the faults are thicker than those on their foot walls, which indicates that the normal faults are syn-sedimentary faults controlling the deposition of the Lower Cretaceous sediments. Meanwhile, thick Upper Jurassic sediments controlled by numerous syn-sedimentary normal faults accumulated in the Western Depression, while only thin Middle–Upper Jurassic sediments were deposited in the Eastern Depression under the control of the boundary syn-sedimentary fault F4 (Liu, 1994, 1997b; Gao & Wang, 2011) (see the cross-section AB in Figs 1 and 3). The aforementioned analysis indicates that faulting subsidence in the Western Depression was more intense than that in the Eastern Depression, and the Central Uplift separated the Eastern Depression from the Western Depression during the late Middle Jurassic – early Late Jurassic Period. It was not until the Early Cretaceous that the two depressions and indeed the entire basin were covered by Cretaceous sediments to form a unified basin.

##### 4.1.2. Reverse faulting and strike-slip faulting during the late Late Jurassic

A NNE-striking level 2 reverse fault and a series of NNE–NE-striking and dominantly NW-dipping level 3 reverse faults and strike-slip faults can be clearly identified below the  $K_1b/J_3f$  unconformity. These faults strongly and synchronously deformed the Lower Palaeozoic–Jurassic strata (Figs 3 and 5). The level 2 fault, the Xilin–Heishantuo fault (see F5 in Fig. 3b), is a high-dip-angle reverse fault and dips to the SE, with dip angles of 45–60° and a vertical fault throw of c. 1500 m. This reverse fault



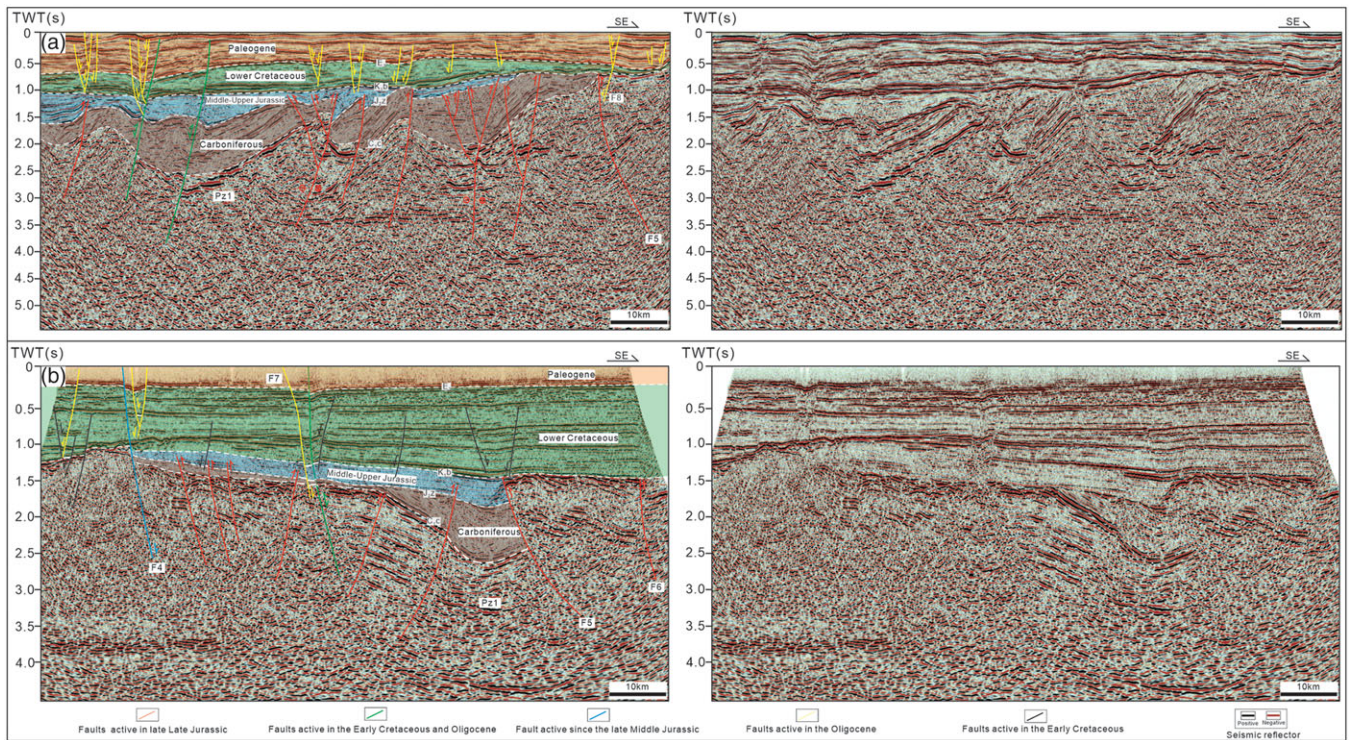


**Fig. 3.** (Colour online) Geological interpretations of two 2D seismic profiles (see Fig. 1c for corresponding locations), showing the characteristics of long-lived normal faults active since the late Middle Jurassic, reverse faults and strike-slip faults active in the late Late Jurassic, normal faults active in the Early Cretaceous, normal faults active in the Oligocene, and inverted reverse faults active in the Early Cretaceous and Oligocene. Also shown are the interpreted strata, i.e. the Carboniferous, Middle–Upper Jurassic, Lower Cretaceous, Oligocene and Quaternary strata.

thus forms both the eastern boundary of the Eastern Depression and the eastern boundary of the residual Carboniferous strata. These aforementioned reverse faults plunge downward into the basement and terminate upward in the Carboniferous strata or at the bottom of the Jurassic strata. The Carboniferous–Jurassic strata on their hanging walls are strongly folded and denuded, and the truncation signature formed at the top of the folds is clearly visible. The faults and strata on their hanging walls are unconformably overlain by Lower Cretaceous strata.

Blocks on both sides of a strike-slip fault typically exhibit characteristics of transtensional or transpressional movements (Harding, 1985; Xia *et al.* 2007; Li *et al.* 2015). Some fault assemblages in the Lower Palaeozoic–Jurassic rocks are interpreted as positive flower structures, indicating local transpressional deformation (Fig. 5d–e). The trunk strike-slip fault plunges into the basement steeply and bifurcates upward into several oblique minor faults, which have the appearance of a flower. The strata are folded and deformed at the top of the flower structure, often forming anticlines, which may also constitute potential traps. From the projection of the strike of the transpressional faults on the strike-slip Mohr strain envelope (Fig. 7a further below), it can be seen that these faults controlling the formation of flower-like structures form a small angle with the principal displacement zone, showing compressional but much stronger strike-slip properties.

The kinematics of the aforementioned reverse faults and strike-slip faults indicate that they were formed by NW–SE compression that may be related to the remote response of the North China Block to the collision and subsequent subduction of the Palaeo Pacific Plate beneath the Eurasian Plate during the Late Triassic–Cretaceous (Dong *et al.* 2019; Zhang & Dong, 2019).

Most of these reverse faults extend upward and terminate in the Upper Jurassic rocks, and the erosion and uplifting of the Upper Jurassic strata indicate thrusting activity related to a NW–SE-trending contraction during the late Late Jurassic. The uplift of the Helan Mountains affected the Mesozoic–Cenozoic tectonic deformation of the adjacent Bayanhaote Basin and Yinchuan Graben, as well as that of the Ordos Basin. Apatite fission track ages indicate that a large-scale top-to-NW fold-thrusting event occurred at the western margin of the Ordos Basin at 160–137 Ma in response to the strong uplifting of the central and northern Helan Mountains during the Middle–Late Jurassic Period (170–140 Ma) (Yang & Dong, 2018; Ma & He, 2019). This intraplate deformation under NW–SE compression may have spread to the Bayanhaote Basin and influenced the fold-thrusting deformation of the Lower Palaeozoic–Jurassic strata in the eastern region of the Bayanhaote Basin. Therefore, combining the records of the faults and unconformities interpreted by seismic data, we infer that the formation period of the aforementioned faults was approximately limited to the late Late Jurassic.

#### 4.1.3. Normal faulting in the Early Cretaceous

A series of NNE–NE-striking normal faults can be clearly identified beneath the  $K_1b/E_3$  unconformity in some seismic profiles (Figs 3b, 6a–c, f). The gently dipping thick Lower Cretaceous strata in the north show good horizontal continuity and are cut by a series of small- to medium-scale high-dip-angle normal faults with small fault throws of 75–375 m (Fig. 3b), while a few normal faults formed during the Early Cretaceous in the southern portion of the depression (Fig. 3a). Some normal faults terminate upward at the top of the Lower Cretaceous rocks and terminate downward at the bottom of the Lower Cretaceous rocks;

Tectonic regime	Diagrams of geometric styles		
Extension			
	Horst	Fault terrace	Fault block (synthetic-antithetic system; master fault on the right)
Extension			
	Graben	Tilted fault block	Fault block (synthetic-antithetic system; master fault on the left)
Compression			
	Back-thrust-ramp assemblages	Faulted anticline (thrust belt)	Faulted anticline (synthetic-antithetic system)
Strike-slip			
	Positive flower structure	Negative flower structure	
Inversion	<p>Denudation plane</p> <p>Early compression</p> <p>Late extension</p>		
	Negative inverted fault		

**Fig. 4.** (Colour online) Classification of structural styles in the Eastern Depression, Bayanhaote Basin, according to kinematic and geometric characteristics (referred to Song *et al.* 1999; Zhang *et al.* 2014; Cheng *et al.* 2016; Liu, 2018).

other normal faults terminate downward in the Carboniferous–Jurassic rocks or even in the Lower Palaeozoic rocks, which affected the deep compressional deformation. Furthermore, a few normal faults exhibit weak syn-sedimentary faulting, which

clearly controlled the deposition of parts of the Lower Cretaceous strata (Fig. 3b). The fold deformation of the Lower Cretaceous rocks was weak, and only small traction bending can be seen locally near a few fault planes.



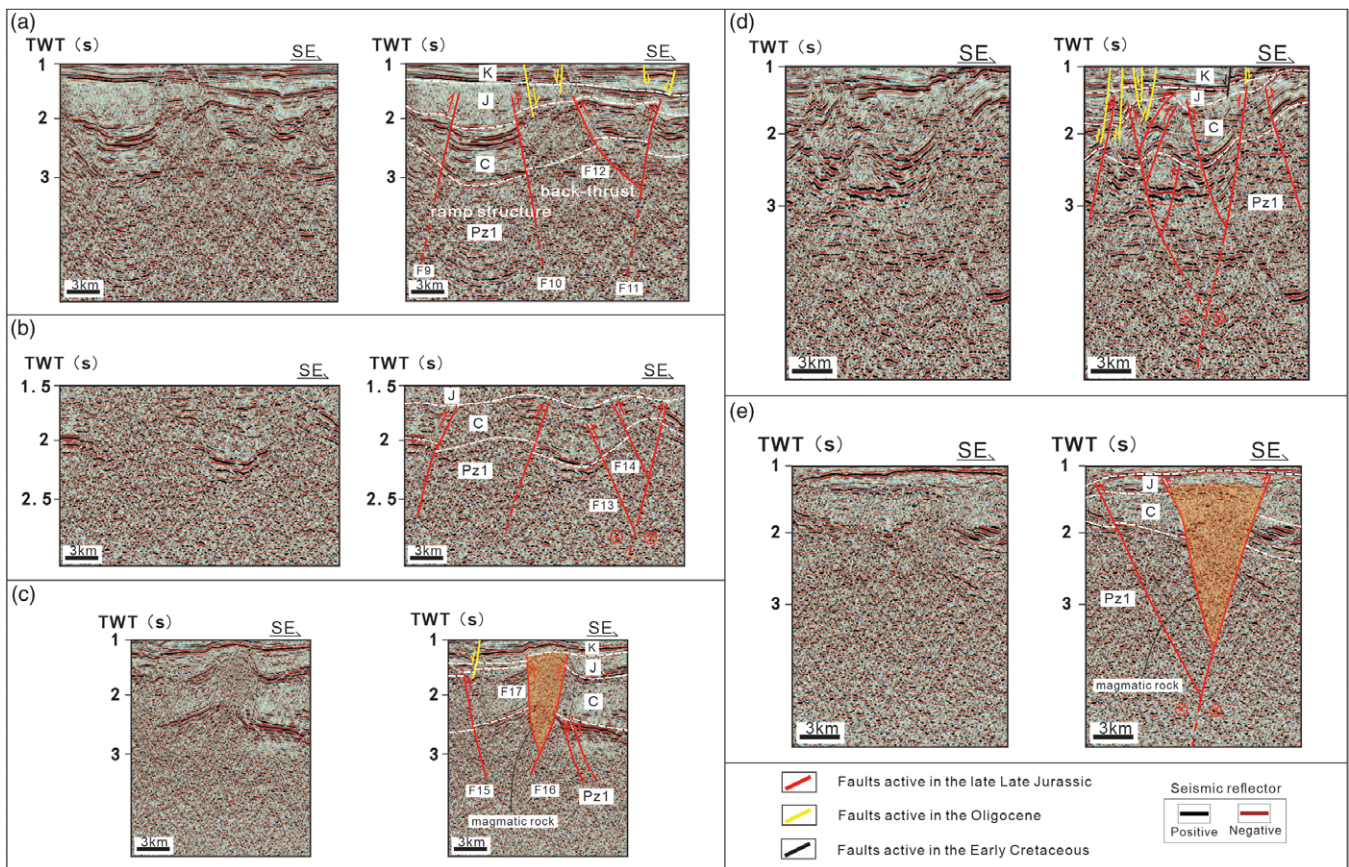


**Fig. 5.** (Colour online) Uninterpreted and interpreted 2D seismic profiles showing the compressional structures and strike-slip structures in the Eastern Depression, Bayanhaote Basin. The compressional structures include (a) the back-thrust – ramp structural assemblages, (b) faulted anticlines (thrust belts) and (c) faulted anticlines with synthetic-antithetic fault systems (see Fig. 1c for the profiles' locations). The strike-slip structures mainly include the positive flower structures (d and e) (see Fig. 1c for the profiles' locations).

#### 4.1.4. Normal faulting in the Oligocene

The high-dip-angle normal faults that formed during the Oligocene and exhibit small displacements can be clearly identified in the seismic profiles from both the northern and the southern parts of the Eastern Depression. In some selected seismic profiles (Figs 3 and 6), most of these small-scale normal faults terminate upward at the top of the Oligocene rocks and terminate downward in the Jurassic or Lower Cretaceous rocks. Meanwhile, some faults branch upward and form a negative flower structure in the leftmost part of the profile, indicating local late-stage transtensional deformation (Figs 3a and 6f). However, in other seismic profiles (Figs 3b, 5d and 6c, f), some large-scale normal faults were formed in the Oligocene and cut the Carboniferous and Lower Palaeozoic rocks, and the deep sequences underwent adjustment by late-stage extension (see F7 and F8 in Fig. 3 and F18 and F19 in Fig. 6).

#### 4.1.5. Negative inverted faulting during the Early Cretaceous and Oligocene

The negative inverted faults cut vertically through nearly all sequences and are found in the Eastern Depression; their presence indicates a tectonic transition from a compressional to an extension regime (Fig 3 and 6a, c). Analysis of the fault throws of all reverse faults indicates that the upper fault throw of some reverse faults is smaller than that of the lower fault throw, whereas some early reverse faults were directly reactivated and showed typical

negative inversion that caused normal faulting of the Lower Cretaceous–Oligocene strata and reverse faulting of the Carboniferous–Jurassic strata (Figs. 3 and 6a, c). This demonstrates that some reverse faults that formed during the early stage were reactivated and inverted in the Early Cretaceous and inherited in the Oligocene. Meanwhile, some normal faults with small displacements were formed during this period and cut the deep sequences. The aforementioned inverted faults and normal faults that cut the deep strata indicate that the deep-lying sequences exhibit adjustment to late-stage extension (Fig. 3b).

## 4.2. Twelve Mesozoic–Cenozoic structural styles

The main structural styles of the Mesozoic–Cenozoic strata in the Eastern Depression can be classified into four major categories according to their formation mechanisms and tectonic regimes (i.e. compression, strike-slip, extension and inversion) and can be further subdivided into 12 geometric styles (Fig. 4). Moreover, an individual geometrical style often contains two or more fault combinations, which originate from multi-stage evolution.

### 4.2.1. Compressional structural style

Compression resulted in various geometric styles including back-thrust – ramp structural assemblages (Fig. 5a), fold and thrust belts (Fig. 5b) and faulted anticlinal structures (Fig. 5c). Back-thrust and



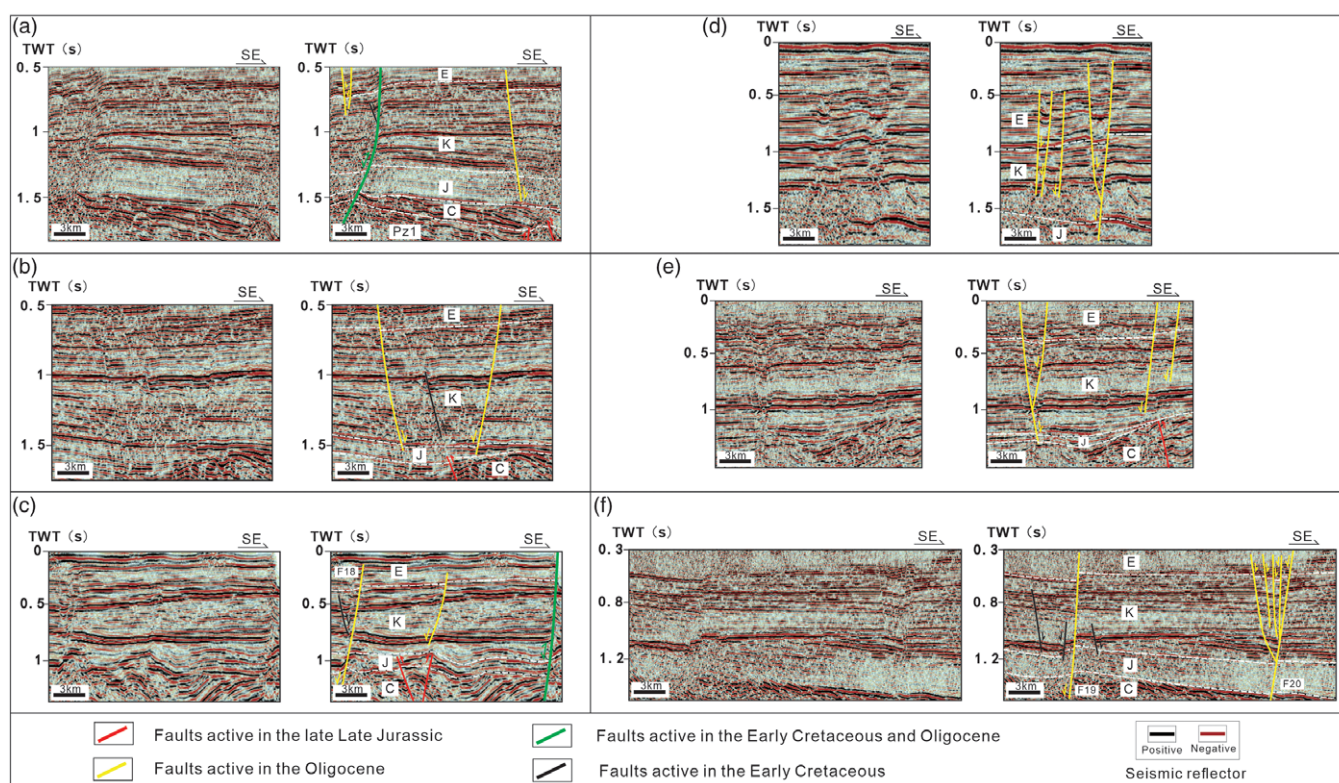


**Fig. 6.** (Colour online) Uninterpreted and interpreted 2D seismic profiles showing the extensional structures in the Eastern Depression, Bayanhaote Basin. The extensional structures include (a) horsts, (b) grabens, (c) fault terraces, (d) a fault block with a major fault on the right and a minor fault on the left, arranged in a synthetic–antithetic system, (e) a fault block with a major fault on the left and a minor fault on the right, arranged in a synthetic–antithetic system, and (f) tilted fault blocks with a locally developed negative flower structure (see Fig. 1c for the profiles' locations).

ramp assemblages are well developed in the study area, with the ramp structure defined by two faults thrusting in the same direction (see F9 and F10 in Fig. 5a) and the back-thrust structure defined by two faults thrusting in opposite directions (see F10 and F11 in Fig. 5a). Back-thrust and ramp structures often occur concomitantly, forming back-thrust – ramp structural assemblages (Fig. 5a). An antithetic minor fault (F12) is observed on the rightmost reverse fault, forming a local faulted anticline. A well-developed thrust belt consisting of three parallel reverse faults dips towards the NW (Fig. 5b), with an anticline usually formed on the hanging wall of the fault. In addition, two minor antithetic faults (see F13 and F14 in Fig. 5b) are seen on the rightmost reverse fault, forming a local positive flower structure. In Figure 5c, the overall structure shown is that of a back-thrust structure controlled by faults F15 and F16, with a fault structure having a major (F16) and an antithetic minor fault (F17) developed in the middle. This means that two faults intersect and their hanging walls are uplifted. Here, we interpret some magmatic rocks, controlled by two reverse faults, which intrude upward into the Carboniferous and Jurassic strata and are covered by the Lower Cretaceous strata. Furthermore, the Lower Cretaceous strata are weakly deformed, forming an anticline. Based on regional tectono-magmatic events, we infer that the emplacement may have occurred along the fault planes during the late Late Jurassic, because the Late Jurassic (158–148 Ma) and Early Cretaceous (142–112 Ma) are two important periods of magmatic activity along the western margin of the North China Block influenced by the Yanshanian movement (Dong *et al.* 2019). However, no further chronological data on the magmatic rocks are available, and this aspect requires further investigation.

#### 4.2.2. Strike-slip structural style

The strike-slip structures in the Eastern Depression can be divided into two categories, i.e. transpressional and transtensional structures. Examples of transpressional structures include the fault assemblages in Figure 5d–e. Faults of this category spread upward and converge downward to form ‘positive flower structures’. In Figure 5e, some seismic reflectors are disordered and discontinuous, and appear to represent intrusive magmatic rocks. The magmatic rocks, which are controlled by the two transpressional faults, intrude upward into the Carboniferous strata and part of the Jurassic strata, and are overlain by the deformed Jurassic and Cretaceous strata. This may imply the existence of magmatic activity in the Late Jurassic. Transtensional structures, which exhibit purely tensional characteristics, are locally developed in the Lower Cretaceous – Oligocene strata, and are depicted in the leftmost parts of Figures 3a and 6f. Faults of this kind converge downward to form a ‘negative flower structure’.

#### 4.2.3. Extensional structural style

On the seismic profiles (Fig. 6), we interpreted many structures related to normal faults trending to the NE, including primarily horsts (Fig. 6a), grabens (Fig. 6b), fault terraces (Fig. 6c) and tilted fault blocks (Fig. 6f). Horsts and grabens are fault block structures formed by homogeneous shear and differential subsidence under biaxial tensile stress. The throws on the normal faults on both sides of the blocks are 150–300 m, and flat horsts and grabens are common. The fault terraces consist of a group of step-down faults developed on a slope, with both the blocks and faults dipping towards the NW (Fig. 6c). The step-down faults consist of a group of normal faults with the same dip, and the inclinations of the strata

differ from the dip of the faults; the tilted fault blocks are well developed in the sections (Fig. 6f). We also interpreted a few structures called synthetic–antithetic fault systems. One type displayed an oblique intersection between a main normal fault on the right and an antithetic minor fault on the left (Fig. 6d) (Cheng *et al.* 2016; Liu, 2018). Another type displayed the switching of fault dips with an oblique intersection between a main normal fault on the left and an antithetic minor fault on the right (Fig. 6e). In general, the extensional structures of the Eastern Depression are dominated by stages of faulting subsidence (Early Cretaceous) and down-warp subsidence (Cenozoic).

#### 4.2.4. Inversion structural style

An inversion structure is defined as a composite structure produced by the movement of a geological body during certain geological periods in the direction opposite to that which generated its original structural characteristics (Wang *et al.* 2001; Chu, 2004; Yu *et al.* 2018). Seismic profiles indicate that the early-stage reverse faults were inverted under the effect of late-stage extension, producing negative inversion structures (Figs. 3 and 6a, c). These faults mainly developed along the early-stage reverse fault planes. Early-stage thrust movement of the faults folded the Carboniferous–Jurassic strata and resulted in the denudation of the Upper Jurassic and the J<sub>3</sub>/K<sub>1</sub> unconformity, and normal movement of these strata occurred during the Early Cretaceous and Oligocene.

### 5. Mesozoic–Cenozoic tectonic evolution

The Mesozoic–Cenozoic evolution of the Eastern Depression is elucidated by applying 2D tectonic restoration, which indicates that the Eastern Depression has experienced complex multi-phase developmental processes with four unconformities, namely, C<sub>1</sub>c/J<sub>2</sub>z, J<sub>3</sub>f/K<sub>1</sub>b, K<sub>1</sub>b/E<sub>3</sub> and E<sub>3</sub>/Q, developed from the Triassic to the Cenozoic (Fig. 7b). Volume conservation is not considered for the two-dimensional tectonic restoration with strike-slip movements, and the restoration results are only discussed as schematic diagrams of the tectonic evolution.

#### 5.1. Triassic–Jurassic tectonic evolution

Drilling and seismic data in the basin revealed an angular unconformity between Carboniferous and the Middle and Upper Jurassic, with the Permian, Triassic and Lower Jurassic strata absent. This indicated that the basin was still undergoing overall uplift and denudation before the Middle Jurassic (Fig. 7b (a)). Subsequently, the thin Middle Jurassic Zhiluo Formation was deposited due to slow local subsidence in the Eastern Depression. During the late Middle Jurassic, the Bayanwula Mountain controlled the faulting subsidence of the Western Depression, and the thick Upper Jurassic Fenfanghe Formation was deposited (Fig. 7b (b)). This was potentially caused by extension of the upper crust resulting from mantle upwelling and subsequent large-scale magmatic activity in the Bayanwula Mountain, owing to the strong NW–SE-trending compression of the Mesozoic Yanshanian movement. Meanwhile, the Central Uplift, which was controlled by two antithetic normal faults, began to undergo uplift and separated the Western Depression from the Eastern Depression. Subsequently, a thin layer of Late Jurassic sediments was deposited in the Eastern Depression and formed an angular unconformity between the pre-Jurassic and the Jurassic strata (Fig. 7b (b)).

During the late Late Jurassic, the Carboniferous–Jurassic strata were folded by numerous NNE–NE-striking reverse faults and a few strike-slip faults with high-dip angles in the Eastern Depression, with the Upper Jurassic strata partly eroded. The Xilin–Heishantuo fault (F5), a level 2 reverse fault thrusting towards the NW, was developed in the east to separate the Eastern Depression from the Eastern Stepped Slope (Fig. 7b (c)), which was probably influenced by the strong uplifting of the Helan Mountains in the eastern part of the basin related to NW–SE-trending contraction in the Middle–Late Jurassic (170–140 Ma) (Zhao *et al.* 2007; Yang & Dong, 2018; Ma & He, 2019). The eastern boundary of the basin was also formed during this period (Tang *et al.* 1990; Liu, 1994; Dong *et al.* 2019). Meanwhile, the Bayanwula Mountain Fault extends far to the north and forms the western boundary fault of both the Bayanhaote Basin and the Hetao Basin to the north. During this period, the Ordos Block pushed northwestward and sinistral shear movement took place between the northern Hetao Basin and the Ordos Block (Tang *et al.* 1990; Song *et al.* 1999). This resulted in obvious sinistral shear of the Bayanwula Mountain Fault in the northern Hetao area, and may have simultaneously caused the Bayanhaote Basin to be affected by the boundary strike-slip movement (see the left inset in Fig. 7a). Judging from the seismic interpretations and regional events, the study area underwent strong compressive and strike-slip deformation during this period, which was the main period of formation of the deep reverse faults and transpressional faults. These faults formed in the early stage primarily constituted compressional structures; the spatial distribution of the strike-slip structures showed obvious variations (Fig. 8a). Thus, we attempt to reasonably explain this based on stress analysis. The sinistral strike-slip strain ellipse of the boundary fault F1 (see the right inset in Fig. 7a) indicates that the dominant trend of the reverse faults in the central and northern parts of the study area falls between the Y fracture and the P fracture; this highlights the sinistral and compressive characteristics of these faults. The sharp angle between the dominant trend of the reverse faults in the southern part and the principal displacement zone is greater; this indicates that the reverse faults in the south have sinistral characteristics, but the compressive nature of these faults is stronger. This may also explain why strike-slip structures were mainly distributed in the central and northern parts of the study area. The strain ellipse indicates the existence of a natural compressive stress in the strike-slip zone (Deng *et al.* 2019). However, because the whole basin was subjected to NW–SE compressive stress ( $\sigma$ ), decomposition of the stress reveals that the basin was not only influenced by strike-slip shear stress ( $\sigma_{\tau}$ ), but that compressive stress ( $\sigma_n$ ) was also superimposed upon it (see the left inset in Fig. 7a). Thus, the Eastern Depression was subjected to strong compressional and shortening deformation, accompanied by the influence of the strike-slip movement of the boundary fault; this resulted in the formation of compressional and strike-slip structures in the Lower Palaeozoic – Jurassic rocks (Fig. 8a).

#### 5.2. Cretaceous tectonic evolution

The intense intracontinental orogeny during the Late Jurassic (i.e. the Yanshanian movement) was followed by large-scale magmatic activity during the Early Cretaceous (Dong *et al.* 2019). In the Early Cretaceous, thick Lower Cretaceous strata were deposited throughout the basin, and some small- to medium-scale NE-striking normal faults with high dip angles were developed and



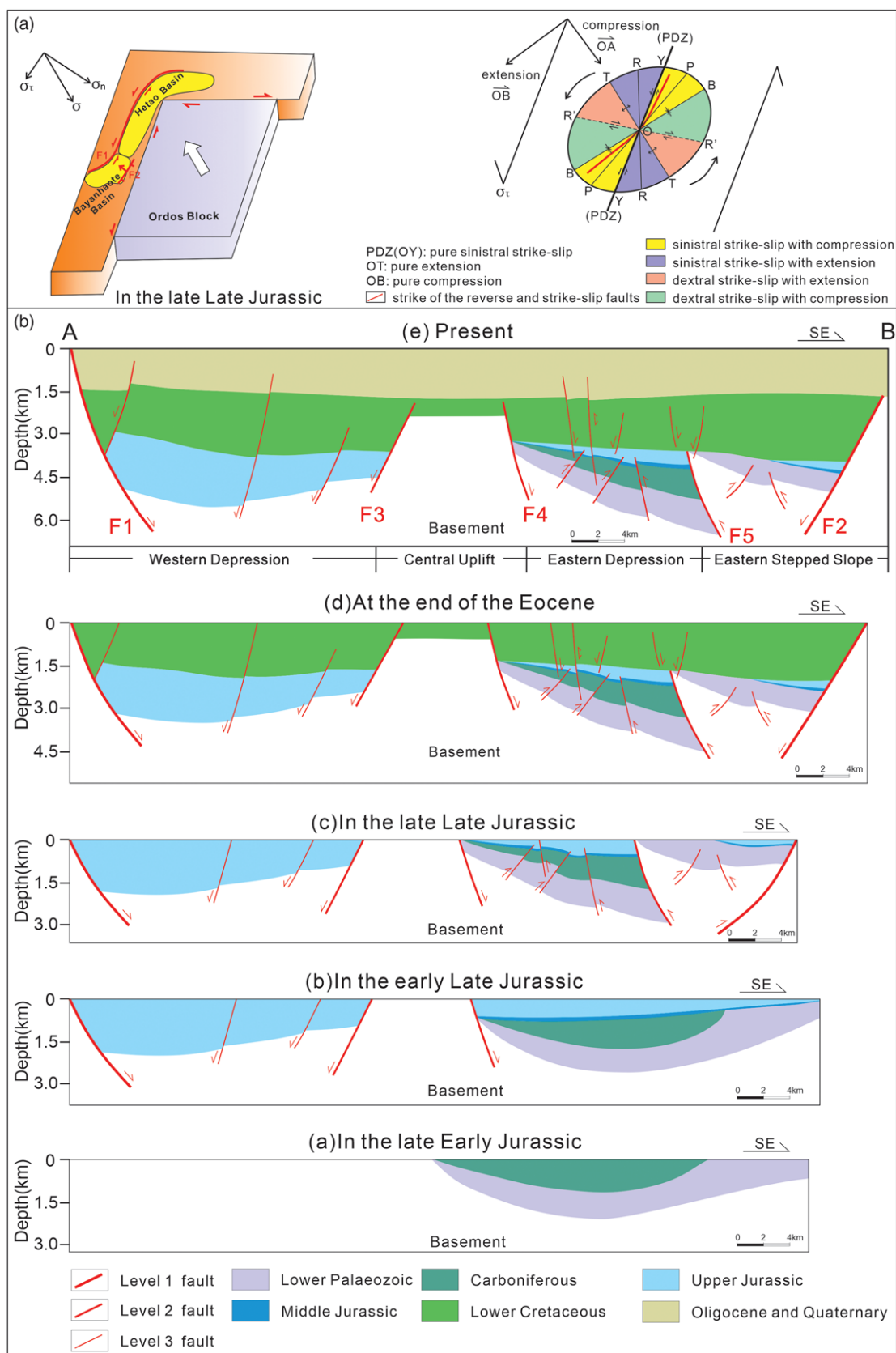


**Fig. 7.** (Colour online) (a) The left inset shows that the Bayanwula Mountain Fault (F1) may be the result of sinistral strike-slip movement during the late Late Jurassic. The right inset shows the sinistral strike-slip strain ellipse of the boundary fault F1, indicating that the fault formed as a result of strike-slip and compressive movements (modified from Deng *et al.* 2019). (b) Tectonic evolution sections of a linked seismic profile AB across the northwestern part of the Eastern Depression, showing that the Eastern Depression and its adjacent structural units have experienced multi-phase Meso-Cenozoic development processes.

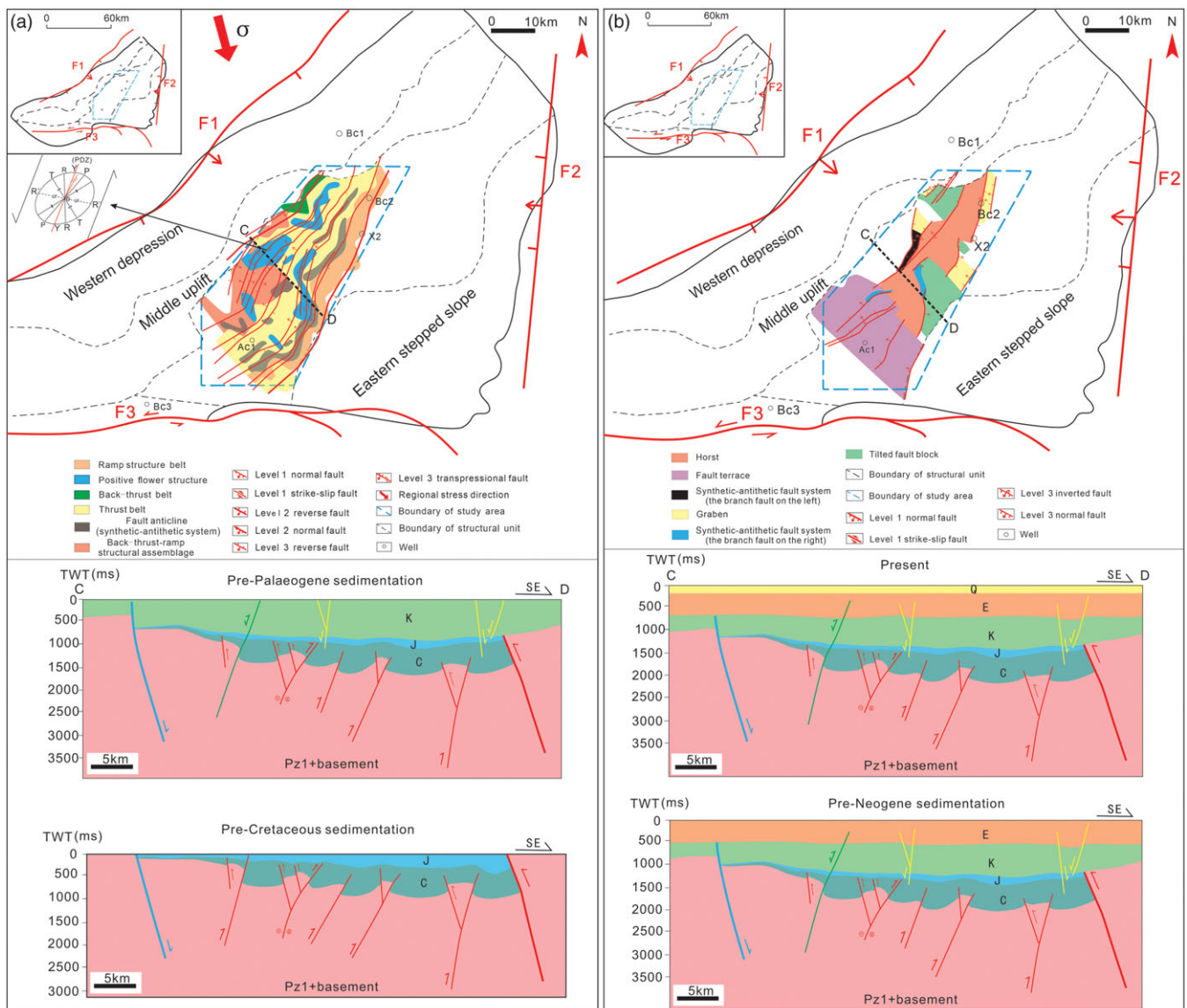


**Fig. 8.** (Colour online) (a) Map of the planar distribution of compressional and strike-slip structural styles in the Lower Palaeozoic – Jurassic rocks in the Eastern Depression, Bayanhaote Basin. Also shown at the bottom is a schematic diagram of the sectional evolution of structural styles during the Jurassic–Cretaceous. (b) Map of the planar distribution of extensional structural styles in the Cretaceous–Quaternary rocks in the Eastern Depression, Bayanhaote Basin. Also shown at the bottom is a schematic diagram of the sectional evolution of structural styles during the Palaeogene–Quaternary.

cut the Jurassic – Lower Cretaceous strata in the Eastern Depression (Fig. 7b (d)). This caused the formation of extensional structures, such as horsts, grabens, fault terraces and tilted fault blocks, in shallow sequences (Fig. 8b). Furthermore, some early-stage reverse faults were directly reactivated and negatively inverted to extend upward to the shallow strata (Fig. 7b (d)). There is substantial geological evidence to indicate that a NW–SE or NWW–SEE-oriented crustal extension occurred around the Bayanhaote Basin, Helan Mountains in the south, and the western Ordos Basin in the Early Cretaceous (Gao *et al.* 2003; Yang *et al.* 2010; Yang & Dong, 2018); this resulted in a peak in magmatic activity (~128 Ma) in and around the North China Block (Dong *et al.* 2019; Zhang & Dong, 2019). This evidence includes the NNE–NE-trending faulting-subsidence basins and stepped normal faults that formed in the Lower Cretaceous rocks

in the western margin of the Helan Mountains; a widely distributed Early Cretaceous NNE–SSW-oriented metamorphic core complex in the Daqingshan area at the western margin of the Ordos Basin (Liu *et al.* 2006); and the occurrence of ~92.6 Ma diabases in well X1, and ~128.26 Ma diabases in well BC3, in the Bayanhaote Basin (Gao & Wang, 2011). The extensional tectonism that formed the aforementioned extensional structures may have been caused by a stress relaxation after strong intracontinental orogeny and an adjustment of the crustal structures of orogenic belts, which was influenced by the collision and subduction of the ancient Pacific Plate beneath the Eurasian Plate (Gao, 2014). During the Late Cretaceous, the Late Yanshanian movement resulted in regional uplift and erosion of the Upper Cretaceous – Eocene strata in the Eastern Depression and caused the Lower Cretaceous to be unconformably overlain by Oligocene strata.



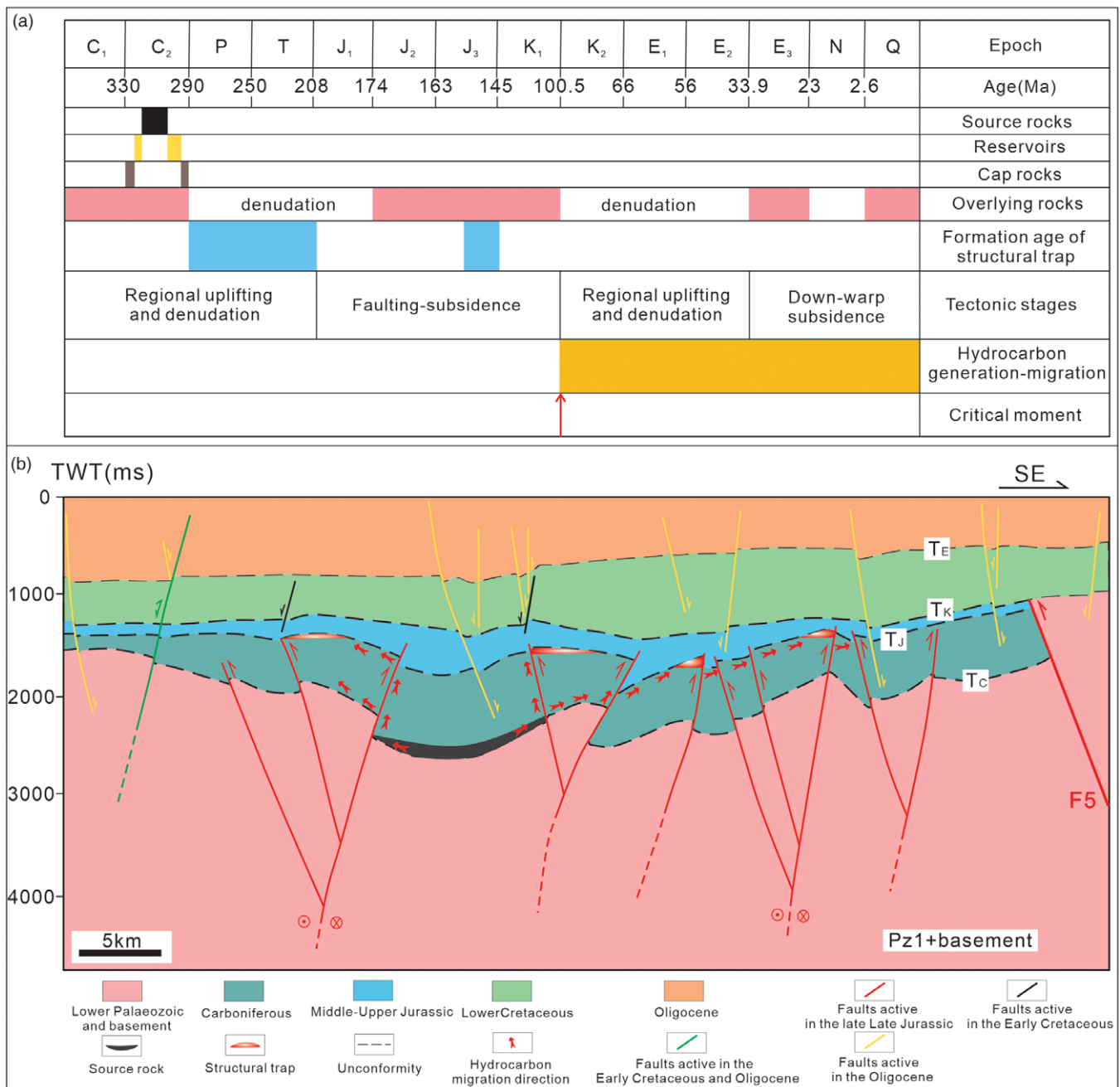


**Fig. 9.** (Colour online) (a) Chart of the petroleum system events in the Eastern Depression, Bayanhaote Basin. It demonstrates the correlation of geological elements in the study area, including the allocation of source rocks, reservoirs and caps; the formation period of structural traps; tectonic deformation stages; hydrocarbon generation and migration periods; and the critical moment showing the beginning of an expulsion of a large amount of hydrocarbons. (b) Diagram of hydrocarbon migration pattern since the Late Cretaceous in the Eastern Depression, Bayanhaote Basin, showing how the hydrocarbons generated from the Carboniferous source rocks primarily migrated along the unconformities and some opening reverse faults and strike-slip faults and accumulated in the potential structural traps (see Fig. 1c for the location of the profile).

**5.3. Cenozoic tectonic evolution**

In the Oligocene, the Eastern Depression continued to subside and thin Oligocene sediments were deposited. Numerous NNE-NE-striking new normal faults were formed and cut the Jurassic, Lower Cretaceous and Oligocene rocks (Fig. 7b (e)). Moreover, some newly formed large-scale normal faults extended downward to the Lower Palaeozoic rocks, adjusting the previous deformation. Furthermore, previous inverted reverse faults were inherited and developed, and continued to show normal faulting. In the Neogene, the entire basin underwent uplift; the Neogene strata

are absent, indicating that no Neogene strata were deposited or that the Neogene strata were eroded. Subsequently, the whole basin remained almost inactive in the Quaternary; a thin layer of Quaternary sediments was deposited and unconformably underlain by the Oligocene strata. Moreover, the existing extensional structural styles were inherited from those in the Cretaceous and remained unchanged as a whole. Since then, this structural framework has been maintained in the Eastern Depression and is visible at present. The record of the aforementioned fault activities indicates a nearly NW–SE extension in the Oligocene, which

**Table 1.** Characteristics of structural styles and potential petroleum traps in the Eastern Depression, Bayanhaote Basin.

No.	Trap type	Structural style	Trap closure height (m)	Trap closure area (km <sup>2</sup> )	Trap formation period	Hydrocarbon expulsion period
1	Faulted anticline	Thrust belt	300	15.2	J <sub>3</sub>	K <sub>2</sub> -Q
2	Faulted anticline	Thrust belt	300	3.5	J <sub>3</sub>	K <sub>2</sub> -Q
3	Faulted anticline	Fault pattern with a major and a minor fault, arranged in a synthetic-antithetic system	450	9.2	J <sub>3</sub>	K <sub>2</sub> -Q
4	Faulted anticline	Fault pattern with a major and a minor fault, arranged in a synthetic-antithetic system	225	7.3	J <sub>3</sub>	K <sub>2</sub> -Q
5	Faulted anticline	Fault pattern with a major and a minor fault, arranged in a synthetic-antithetic system	375	10.3	J <sub>3</sub>	K <sub>2</sub> -Q
6	Faulted anticline	Thrust belt	450	23.4	J <sub>3</sub>	K <sub>2</sub> -Q
7	Faulted anticline	Thrust belt	225	14.8	J <sub>3</sub>	K <sub>2</sub> -Q
8	Anticline	Positive flower structure	300	10.2	J <sub>3</sub>	K <sub>2</sub> -Q
9	Anticline	Positive flower structure	150	1.4	J <sub>3</sub>	K <sub>2</sub> -Q

was an important period for the reactivation of shallow normal faults and some deep reverse faults and the formation of the large-scale normal faults that cut the deep strata in the Eastern Depression. These dynamics probably result from the collision and orogeny between the Indian and Eurasian Plates since the Eocene (55 Ma), which caused the extrusion and uplift of the Tibetan Plateau to the northeast (Zhang *et al.* 2006). As a result of the influence of its remote response, the Helanshan Tectonic Belt to the east and its adjacent regions were compressed by a NNE-SSW regional compressional stress (Zhang *et al.* 2006; Gao, 2014; Yang & Dong, 2018; Ma & He, 2019). Differential uplift occurred in various regions of the Helan Mountains, which directly led to the inversion of early reverse faults at the eastern margin of the Helan Mountains and the formation of the Yinchuan Graben; this differential uplift also caused the infilling of the Yinchuan Graben and the Bayanhaote Basin with Oligocene sediments (Yang & Dong, 2018; Ma & He, 2019). The NNE-striking Helan Fault (F2) probably simultaneously underwent normal faulting, and this controlled the formation of the Oligocene secondary normal faults and the inversion of early reverse faults in the Eastern Depression. Furthermore, the continuous activity of the Tibetan Plateau during 23–20 Ma probably caused the Oligocene strata to be unconformably overlain by Quaternary strata.

#### 5.4. Distribution characteristics of Mesozoic-Cenozoic structural styles

Based on the planar view (Fig. 8), the structures are distributed in NE-trending strips. Back-thrust – ramp structural assemblages developed in the western region of the study area during the Lower Palaeozoic – Jurassic (see the lower inset in Fig. 8a). Thrust belts developed in the central part of the study area, and positive flower structures developed owing to the influence of faults with a strong transpressional component. In the east, the ramp belts are the main structures; they consist of a major and a minor fault arranged locally in a synthetic-antithetic system. Fault terraces developed in the southern portion of the study area during the Cretaceous-Quaternary interval (see the lower inset in Fig. 8b), and the central horsts developed in alternating fashion with the graben in the eastern part, and the tilted fault blocks in the northern and southeastern parts, of the study area. At the end of the Middle Jurassic, the entire basin was subjected to

NW-SE compressional stress. However, the central and western parts of the study area were more significantly affected by the orogeny of the western Bayanwula Mountain, resulting in the formation of thrust faults eastward. Simultaneously, at the western margin, back-thrust – ramp structural assemblages regulated by some antithetic faults were formed. The eastern margin of the study area may have been influenced by the orogeny of the Helan Mountains (F2) to form a thrust fault westward and consequently form the ramp belt. Owing to the stronger strike-slip behaviour in the north, the strike-slip structures are mainly distributed in the central and northern parts of the study area.

## 6. Prediction of petroleum traps

### 6.1. Hydrocarbon generation and migration conditions

Analysis of the petroleum system events in the study area (Fig. 9a) indicates that the Eastern Depression has a good source-reservoir-cap configuration and favourable migration and accumulation conditions (Fig. 9b). The Carboniferous rocks are the main source rocks in the Eastern Depression. Three types of source rocks, namely dark mudstone, limestone and coal seams, have developed, with the dark mudstone having the highest organic matter content and the greatest hydrocarbon generation potential (Wei & Tan, 2009; Li *et al.* 2013). The thicknesses of the dark mudstones in the Jingyuan and Yanghugou formations are 246 m and 250 m, respectively, as identified in well BC2. The thickness of the Carboniferous source rock in well AC1 is *c.* 365 m. The organic matter in the dark mudstone mainly consists of type II2 and type III organic matter, and dark mudstone is mature to over-mature (A Li *et al.* 2013; YN Li *et al.* 2017). The lithology of the Carboniferous reservoir consists of interbedded sandstone, mudstone and siltstones. The average porosity is 5.77 %, and the average permeability is  $0.75 \times 10^{-3} \mu\text{m}^2$ , which provides sufficient reservoir space (Wei *et al.* 2008; Wang & Huang, 2014; Sheng, 2019).

The Carboniferous source rocks began to generate large amounts of hydrocarbons at the end of the Late Cretaceous and are currently at the peak of hydrocarbon generation. The basin was characterized by late hydrocarbon accumulation, and the migration of oil and gas mainly occurred after the Eocene (Xiong *et al.* 2000; Cao *et al.* 2001, 2003). The upper surface of



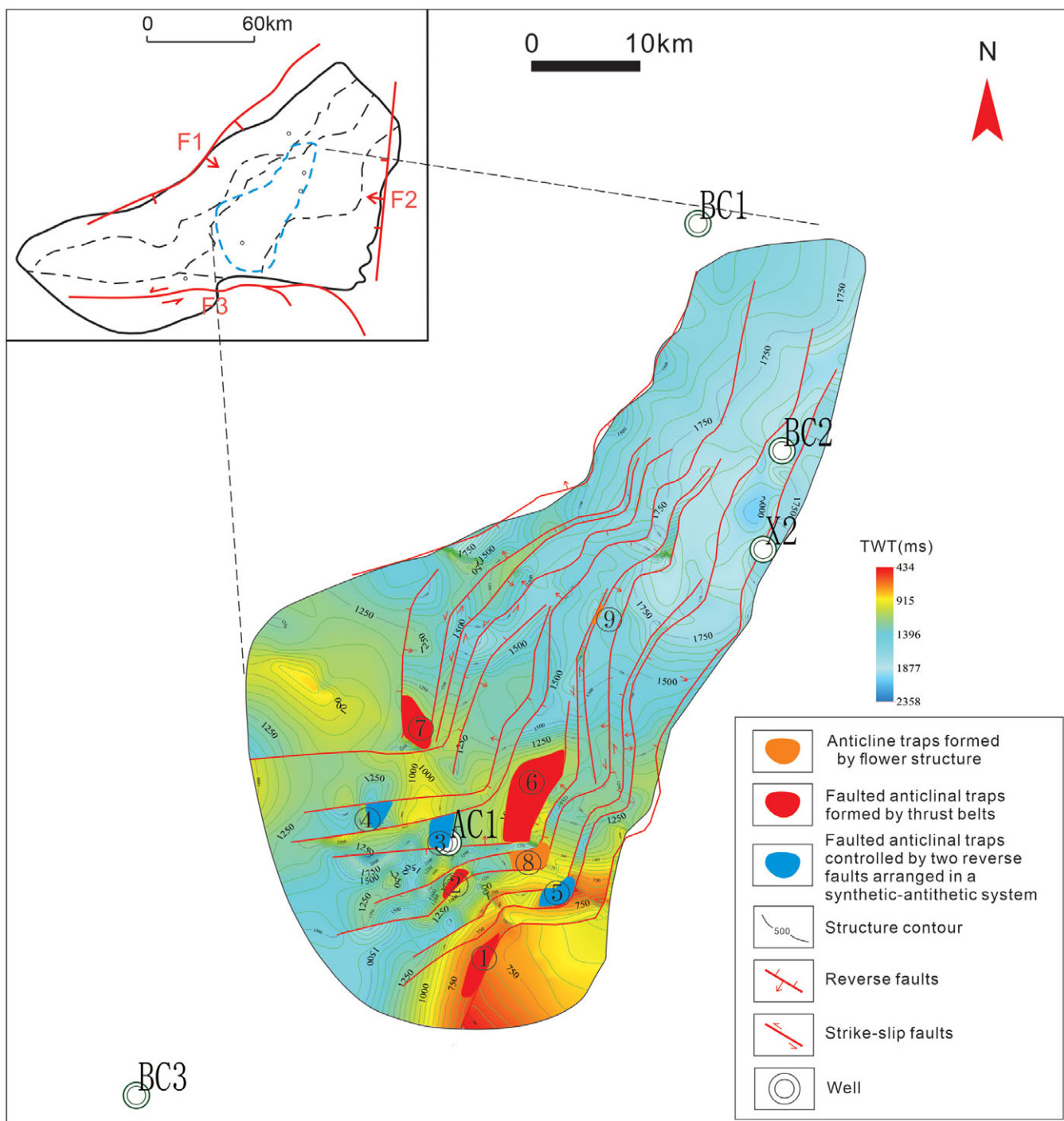


**Fig. 10.** (Colour online) Map of the location of Carboniferous structural traps in the Eastern Depression, Bayanhaote Basin. The potential structural traps are mainly faulted anticlines distributed around well AC1.

the Lower Palaeozoic strata and the bottom surface of the Jurassic strata are important regional unconformities in this area. Carbonate weathering crusts are well developed along these unconformities, both of which were primary lateral migration channels for hydrocarbons and are important reservoirs (Xiong *et al.* 2000; Gao & Wang, 2011). The reverse faults may have served as channels for the vertical or lateral migration of hydrocarbons (Fig. 9b). The Carboniferous mudstone has a strong sealing ability,

and the Lower Cretaceous mudstone found in well X2 is presumed to possess sealing ability.

### 6.2. Controls of structural styles on petroleum trapping

The shallow strata were mildly deformed by the late-stage extension, and the gently dipping strata and small scale of the normal faults in the shallow strata resulted in poor trap development.

Compressional and strike-slip structures were formed, with various structural traps developed in the Carboniferous–Jurassic rocks, during the Late Jurassic. Although part of the Upper Jurassic strata was eroded by regional uplift during the latter stage of the Late Jurassic, the traps in the Carboniferous rocks were preserved almost undamaged. The late-stage extensions in the Early Cretaceous and Cenozoic caused the formation of some new normal faults, which extended to the deep strata, but these normal faults were not commonly developed in the anticline area, and the previous traps were therefore well preserved. Moreover, the inversion of reverse faults caused by the late-stage extension may have opened the fault planes of some reverse faults and facilitated the vertical migration of deep oil and gas to fill the traps. Thrust belts, faulted anticlinal structures and positive flower structures are considered to be the most favourable structural styles for petroleum trapping. Based on the number of structural traps in the Carboniferous rocks (Table 1), three types of favourable structural traps were formed, as shown in Figure 10. These are mainly fault-related anticlines controlled by different structural patterns. Note that for all styles, the trap formation period was the Late Jurassic ( $J_3$ ), and the hydrocarbon expulsion period was the Late Cretaceous ( $K_2$ ) – Quaternary (Q).

Under the control of the central thrust belts, many faulted anticlines were formed in the Carboniferous rocks. The scale of these traps varies owing to the different degrees of compression. Four faulted anticlines on the thrust belts that developed within the study area have closure heights of 225–450 m and closure areas of 3.5–23.4 km<sup>2</sup>. There are also many fault structures with a major and a minor fault, arranged in a synthetic–antithetic system, which are secondary structures that developed on the back-thrust and thrust belt in the Carboniferous rocks. Three faulted anticlines controlled by such structures were developed in the study area, with closure heights of 225–450 m and closure areas of 7.3–10.3 km<sup>2</sup>. In addition, the positive flower structures form anticlinal traps through transpression. Two such anticlinal traps were developed in the study area, with closure heights of 150–300 m and closure areas of 1.4–10.2 km<sup>2</sup>.

As a result of this analysis, the locations of nine potential traps have been identified. These traps are controlled by NE-striking reverse faults and strike-slip faults, and they are mainly distributed near well AC1 in the southwestern portion of the study area (Fig. 10). Drilling results show that well AC1 was drilled into Carboniferous dark mudstone with maturity ( $R_o$ ) reaching 0.95–1.07%. A total of five oil- and gas-bearing formations with a total thickness of 27.4 m were identified with some gas shows. Good source – reservoir – cap-rock and migration conditions indicate that these traps are the targets with the greatest exploration potential in the study area.

## 7. Conclusions

Based on the temporal development and structural styles of faults, five types of faults that were active during different stages of the Meso-Cenozoic in the Eastern Depression of Bayanhaote Basin have been defined: long-lived normal faults active since the late Middle Jurassic; reverse faults and strike-slip faults active in the late Late Jurassic; normal faults active in the Early Cretaceous; normal faults active in the Oligocene; and negative inverted faults active in the Early Cretaceous and Oligocene. These Meso-Cenozoic fault assemblages are characterized by four kinematic styles, namely, compression, strike-slip, extension and inversion.

The compressional and strike-slip structures were formed in the late Late Jurassic and were found mainly within the Lower Palaeozoic – Jurassic rocks, while the extensional structures were formed during the Early Cretaceous – Cenozoic, and were found mainly within the Lower Cretaceous – Cenozoic rocks. The late-stage extension influenced and adjusted the deep sequences, with some reactivated and inverted reverse faults and large-scale normal faults forming in the Early Cretaceous and Oligocene and cutting through nearly all cap-rock strata. The structural styles are generally distributed in NE-trending strips and are controlled by NE-striking faults. The final structural pattern in the deep deformed strata ( $P_{Z1-}$ ) consists primarily of back-thrust – ramp structural assemblages in the west, thrust belts in the central part, and ramp structures in the east. The final structural pattern in the shallow deformed strata (K–Q) consists primarily of fault terraces in the south, horsts in the central part, and tilted fault blocks in the east.

The thrust belts, faulted anticlinal structures and positive flower structures control various faulted anticlinal traps in the Carboniferous rocks. Regional unconformities at the bottom of the Jurassic and Carboniferous strata and inverted faults reactivated by late-stage extension provide good vertical and lateral channels for the accumulation of the Carboniferous petroleum in the traps. These traps are mainly distributed near well AC1 in the southwestern region of the study area and are predicted to have the greatest exploration potential.

**Acknowledgements.** This research was supported by the National Natural Science Foundation of China (Grant no. 42072173) and the National Science and Technology Major Project of China (2016ZX05046-003-001). We are grateful to Ruifeng Zhang and other leaders of the PetroChina Huabei Oilfield Company for providing and supporting the data. We also gratefully acknowledge the editors and reviewers for constructive suggestions.

**Declaration of interest.** The authors declare that we have no known competing financial interests or personal relationships that could have appeared to influence the work reported in this paper.

## References

- Allen MB, Macdonald DIM and Xun Z (1997) Early Cenozoic two-phase extension and late Cenozoic thermal subsidence and inversion of the Bohai Basin, northern China. *Marine and Petroleum Geology* **14**, 951–72.
- Cao DY, Liu SY, Zhang SR, Li LY and Cheng GY (2003) Hydrocarbon-bearing prospect evaluation of Carboniferous from Hexi corridor to Bayan Haote basin. *Northwestern Geology* **36**, 62–9.
- Cao XY, Yan YX, Lin XQ, Li YY, Cheng XS and Zhou YX (2001) Discussion on thermal evolution history of the Carboniferous in the Bayanhaote Basin by apatite fission track. *Petroleum Geology and Engineering* **15**, 9–12.
- Cheng YF, Ding WL and Yang C (2016) Study on Permo-Carboniferous structural style and distribution pattern in Wenan slope, Central Hebei depression. *Coal Geology of China* **28**, 1–8.
- Chu XZ (2004) A review of inversion structures in petroliferous basins. *J xi'an Univ Pet (natural science edition)* **19**(1), 28–33.
- Deng H, Li GY, Yang HF, Wen HL and Zhang C (2019) Improvement and application of Riedel shear system. *Advances in Earth Science* **34**, 868–78.
- Dong SW, Zhang YQ, Li HL, Shi W, Xue HM, Li JH, Huang SQ and Wang YC (2019) The Yanshan orogeny and late Mesozoic multi-plate convergence in East Asia: commemorating 90 years of the ‘Yanshanian Orogeny’. *Science China Earth Sciences* **61**, 1888–909.
- Fan CH, Li H, Qin QR, He S and Zhong C (2020) Geological conditions and exploration potential of shale gas reservoir in Wufeng and Longmaxi Formation of southeastern Sichuan Basin, China. *Journal of Petroleum Science and Engineering* **191**, 107–38.

- Gao BS and Wang G** (2011) Evolution characteristics and petroliferous evaluation in Bayanhaote Basin. *Journal of Chongqing University of Science and Technology: Natural Science Edition* **13**, 22–5.
- Gao SH** (2014) *Mesozoic and Cenozoic tectonic evolution of the transverse structure in the middle of western margin of Ordos basin and its significance to oil and gas accumulation*. Master degree thesis, Northwest University, Xi'an, China, —85 pp. Published thesis.
- Gao SL, Li F, Li TB, Lv CG and Lu YJ** (2003) Discussion of the relationship between coal metamorphism and the Late Mesozoic basalt in Rujigou area. *Coal Geology and Exploration* **31**, 8–10.
- Harding TP** (1985) Seismic characteristics and identification of negative flower structures, positive flower structures, and positive structural inversion. *Bulletin of the American Association of Petroleum Geologists* **69**, 582–600.
- Harding TP and Lowell JD** (1979) Structural styles, their plate tectonic habitats and hydrocarbon traps in petroleum provinces. *Bulletin of the American Association of Petroleum Geologists* **63**, 1016–58.
- Hickman RG, Varga RJ and Altany RM** (2009) Structural style of the Marathon thrust belt, West Texas. *Journal of Structural Geology* **31**, 900–9.
- Li A, Huang WH, Yan DN and Gong YY** (2013) Accumulation conditions of the Carboniferous shale gas in Bayanhaote Basin and its southern periphery. *Journal of Xi'an Shiyou University (Natural Science Edition)* **28**, 34–41 + 7–8.
- Li MG, Wu KQ, Kang HQ, Jia HC and Cheng T** (2015) Characteristics of strike-slip structural deformation and distribution of traps formed. *Special Oil and Gas Reservoir* **22**, 44–7 + 152–3.
- Li YN, Peng ZC and Dai YY** (2017) Evaluation of hydrocarbon potential of Carboniferous system in Bayanhot basin. *Petrochemical Industry Application* **36**, 71–7.
- Liu CY, Zhao HG, Gui XJ, Yue LP, Zhao JF and Wang JQ** (2006) Space-time coordinate of the evolution and reformation and mineralization response in Ordos basin. *Acta Geologica Sinica* **80**, 617–38.
- Liu JH, Zhang PZ, Zheng DW, Wan JL, Wang WT, Du P and Lei QY** (2010) Pattern and timing of late Cenozoic rapid exhumation and uplift of the Helan Mountain, China. *Science China Earth Sciences* **53**, 345–55.
- Liu SF** (1998) The coupling mechanism of basin and orogen in the western Ordos Basin and adjacent regions of China. *Journal of Asian Earth Sciences* **16**, 369–83.
- Liu SP and Liu XF** (2002) Structural type of Bayanhaote basin. *Journal of Southwest Institute of Petroleum* **24**, 24–7.
- Liu XF** (1994) Structural characteristics and preliminary evaluation of hydrocarbon potential in Bayanhaote basin. *Journal of Southwest University of Petroleum (Natural Science Edition)* **16**, 18–27.
- Liu XF** (1997a) The study on tectonic evolution history of Western Depression Belt in Bayanhot Basin. *Fault-Block Oil and Gas Field* **4**, 15–8.
- Liu XF** (1997b) Discussion for origin and hydrocarbon potential of the Central Uplift in Bayanhot Basin. *Petroleum Geology and Engineering* **11**, 1–4 + 59.
- Liu XF and Liu SP** (1997) Subsidence history analysis of Bayanhot Basin. *Journal of Xi'an Shiyou University (Natural Science Edition)* **12**, 25 + 5 + 26–31.
- Liu ZH** (2018) Analysis of structural styles in Huangqiao area of Lower Yangtze River. *Petroleum Geology and Experiment* **40**, 502–8.
- Lu JC, Chen GC, Wei XY, Li YH and Wei JS** (2011) Carboniferous–Permian sedimentary formation and hydrocarbon generation conditions in Ejin Banner and its vicinities, western Inner Mongolia: a study of Carboniferous–Permian petroleum geological conditions (part 1). *Geological Bulletin of China* **30**, 811–26.
- Ma JH and He DF** (2019) Meso-Cenozoic tectonic events in the Helanshan Tectonic Belt and its adjacent areas: constraints from unconformity and fission track data. *Acta Petrologica Sinica* **35**, 1121–42.
- Missenard Y, Taki Z, De Lamotte DF, Benammi M, Hafid M, Leturmy P and Sebrier M** (2007) Tectonic styles in the Marrakesh High Atlas (Morocco): the role of heritage and mechanical stratigraphy. *Journal of African Earth Sciences* **48**, 247–66.
- Nieuwland DA, Oudmayer BC and Valbona U** (2001) The tectonic development of Albania: explanation and prediction of structural styles. *Marine and Petroleum Geology* **18**, 161–77.
- Polonia A and Camerlenghi A** (2002) Accretion, structural style and syncontractional sedimentation in the Eastern Mediterranean Sea. *Marine Geology* **186**, 127–44.
- Saqab MM and Bourget J** (2015) Structural style in a young flexure-induced oblique extensional system, north-western Bonaparte Basin, Australia. *Journal of Structural Geology* **77**, 239–59.
- Sepehr M and Cosgrove JW** (2004) Structural framework of the Zagros fold thrust belt, Iran. *Marine and Petroleum Geology* **21**, 829–43.
- Sheng SZ** (2019) Reservoir characteristics of Carboniferous system in Bayanhaote Basin. *Liaoning Chemical Industry* **48**, 297–9.
- Sherkatia S and Letouzey J** (2004) Variation of structural style and basin evolution in the central Zagros (Izeh zone and Dezful Embayment). *Marine and Petroleum Geology* **21**, 535–54.
- Song GQ, Ma YC, Liu CC, Sun QR, Yu MD and Han YJ** (1999) Structural style analysis and its significance in Bayanhaote Basin. *Petroleum Geology and Engineering* **13**, 8–11 + 14–59.
- Tang XY, Feng Q and Li DS** (1990) Tectonic characteristics and evolution of Bayanhaote basin in western Inner Mongolia. *Petroleum and Natural Gas Geology* **11**, 127–35.
- Tripodi V, Muto F and Critelli S** (2013) Structural style and tectono-stratigraphic evolution of the Neogene-Quaternary Siderno Basin, southern Calabrian Arc, Italy. *International Geology Review* **55**, 468–81.
- Wang TH, Wang GH and Zhao ZJ** (2001) Inversion structural styles and hydrocarbon accumulation of petroliferous basins in China. *Marine Origin Petroleum. Geology* **6**, 27–37.
- Wang YQ and Huang K** (2014) Research on sandstone reservoir characteristics of Carboniferous in Banyanhot Basin. *Science and Technology in Western China* **13**, 39–41.
- Wei PS and Tan KJ** (2009) Characteristics and estimate of Carboniferous source rocks in Bayehot basin. *Petroleum Geology and Experiment* **31**, 616–21.
- Wei PS, Tan KJ and Wei ZT** (2008) Carboniferous reservoir features and diagenesis, Bayanhot basin. *Natural Gas Geoscience* **19**, 581–6.
- Xia YP, Liu WH, Xu LG and Zheng LH** (2007) Identification of strike-slip faults and their significance in petroleum geology. *Petroleum Geology* **12**, 17–23.
- Xiong BX, Chen WX, Chen WL and Cao XY** (2001) Formation and evolution of the Bayanhaote prototype basins. *Petroleum Geology and Experiment* **23**, 19–23.
- Xiong BX, Sun ZM, Xiao B, Qi YS and He HQ** (2000) Carboniferous petroleum system and its analysis of potential belt in the Bayanhaote basin. *Geoscience* **14**, 46–51.
- Xu NZ and Gao C** (2020) Study on the special rules of surface subsidence affected by normal faults. *Journal of Mining and Strata Control Engineering* **2**, 101–6.
- Xue MW, Zhang T, Ding WL, Jiao BC, Zhou ZC and Du XY** (2020) Fluid potential characteristics of Carboniferous and the division of hydrocarbon migration and accumulation units in the Eastern Depression of the Bayanhaote Basin. *Journal of Geomechanics* **26**, 65–73.
- Yang H, Fu JH, Ouyang ZJ, Sun LY and Ma ZR** (2010) U–Pb zircon dating of the Daling–Gugutai basalt in Rujigou on the western margin of Ordos Basin. *Acta Geoscientia Sinica* **31**, 229–36.
- Yang KS** (2006) *Seismic interpretation for structures of petroliferous basins in China*. Beijing: Petroleum Industry Press, 614 pp.
- Yang XY and Dong YP** (2018) Mesozoic and Cenozoic multiple deformations in the Helanshan Tectonic Belt, Northern China. *Gondwana Research* **60**, 34–53.
- Yao C, Jiao GH and Wang TH** (2004) *Petroleum-bearing structural styles in China*. Beijing: Petroleum Industry Press, —517 pp.
- Yu ZH, Xiao KY, Zhang GL, Xiao GJ and Du YB** (2018) Analysis on inverted structure characteristics and its forming mechanism in the Bongor Basin, Chad. *China Petroleum Exploration* **23**(3), 90–98.
- Zhang HJ, Huang ZD, Zhou TS, Zhou JH, Cheng YD and Zhang L** (2014) Structural style and hydrocarbon accumulation in southern fault zone of Gaoyou depression. *Journal of Petroleum and Natural Gas* **36**, 51–5.
- Zhang PZ, Zheng DW, Yin GM, Yuan DY, Zhang GL, Li CY and Wang ZC** (2006) Discussion on Late Cenozoic growth and rise of northeastern margin of the Tibetan Plateau. *Quaternary Sciences* **26**, 5–13.



- Zhang YQ and Dong SW** (2019) East Asia multi-plate convergence in Late Mesozoic and the development of continental tectonic systems. *Journal of Geomechanics* **25**, 613–41.
- Zhao HG, Liu CY, Wang F, Wang JQ, Li Q and Yao YM** (2007) Timing of uplift and evolution of the Helan Mountain. *Scientia Sinica Terrae* **37**(S1), 185–92.
- Zhao XC, Liu CY, Wang JQ, Zhao Y, Wang L and Zhang QH** (2016) Detrital zircon U-Pb ages of Paleozoic sedimentary rocks from the eastern Hexi Corridor Belt (NW China): provenance and geodynamic implications. *Sedimentary Geology* **339**, 32–45.
- Zhou JS, Wang NX, Zhao QP, Yin X, Lin GF, Cao Y, Li YY and Han XQ** (2014) Natural gas accumulation characteristics in the upper Paleozoic in the Yanchang exploration block of southeastern Ordos Basin. *Natural Gas Industry* **34**, 34–41.
- Zhou ZC, Ding WL, Zhang RF, Yan DP, Jiao BC, Wu CL, Liu TS, Du XY and Xue MW** (2021) Structural styles and tectonic evolution of Cretaceous to Cenozoic faults in the Linhe Depression of Hetao Basin, China: implications for petroleum traps. *International Journal of Earth Sciences (Geologische Rundschau)* **110**, 2805–29.